EUMETSAT Satellite Application Facility on
Support to Operational Hydrology and Water Management

Algorithm Theoretical Baseline Document (ATBD) for product H64 P-AC-SM2RAIN

Precipitation/Soil Moisture integrated product

Reference Number:	SAF/HSAF/ATBD-64
Issue/Revision Index:	2.1
Last Change:	16 February 2022

Revision History

Revision	Date	Author(s)	Description
1.0	06/12/2019	Luca Ciabatta, Luca Brocca	First draft
2.0	05/05/2020	Luca Ciabatta, Luca Brocca, Christian Massari	Added details about calibration, integration technique
2.1	02/16/2022	Luca Ciabatta	Added details about calibration

Table of contents

List of Figures

1 Executive summary

The Algorithm Theoretical Baseline Document (ATBD) provides a detailed description of the algorithm used to estimate rainfall from soil moisture (SM) data and to merge it with Passive Microwave (PMW) rainfall estimates. SM2RAIN (*Brocca et al., 2013*) is an algorithm which inverts the soil water balance equation to estimate rainfall. The algorithm is here applied to ASCAT SM observations (H SAF products H16 and H101) to obtain H101- and H16-based rainfall estimates which are then merged with the PMW-only H23 product (*Marra et al., 2015*, *Panegrossi et al 2014, 2016, Ciabatta et al., 2017*). The algorithm is implemented in the MATLAB programming language.

2 Introduction

2.1 Purpose of the document

This ATBD is intended to provide a detailed description of the scientific background and theoretical justification for the algorithm used to obtain the merged product.

2.2 Related H SAF products

H64 product is based both on surface SM products (H16, H101 and their successors) and on MW-based daily rainfall estimates (H23). For further information on the SM parent products and retrieval algorithm, the user is referred to the respective ATBDs [*ATBD, 2016*]. H23 is an auxiliary product which provides daily precipitation estimates by combining PMW precipitation rate estimates derived from conical and cross-track scanning radiometers. Specifically, H23 is based on merged MW precipitation rate estimates provided by H01, and H02B (Mugnai et al., 2013, Casella et al., 2013, Sanò et al., 2013). H23 will be replaced by H67 when operational, which will incorporate also precipitation rate estimates provided by H18 (Sanò et al., 2015), and by the auxiliary modules H-AUX-17 (Casella et al., 2017), and H-AUX-20 (Sanò et al., 2016). Further information about these two products can be found in the respective ATBDs [*ATBD, 2013a* and *ATBD, 2013b*]. The H23 algorithm is based on two modules:

1. *remapping module;*
2. *ensemble mean module;*

The remapping module performs bilinear interpolation of the instantaneous precipitation rate in the original orbital (irregular) grid to remap them on a regular 0.25°x0.25° grid.
The ensemble mean module runs every day at 06 UTC and performs an ensemble mean of all the remapped rainfall rate estimates produced from H01 and H02B in the previous day.

2.3 State-of-the-art

It is well known that satellite PMW retrievals provide reliable estimates of rainfall and represent a valuable tool to develop hydrological applications over scarcely instrumented areas. However, the satellite rainfall estimates suffer from different errors (Ebert et al. 2007). The retrieval is impacted by issues in the estimation of light rainfall that cause a general underestimation of the total amount of water and by the indirect nature of measurement that is based on the interaction of radiation with the hydrometeors (*Kidd and Levizzani, 2011*). Due to the instantaneous nature of measurement, the quality and reliability of the estimates rely also on the number of satellite observations contributing in the rainfall estimation. In this respect, the use of constellation of sensors can mitigate this issue (Skofronick-Jackson et al., 2017, Panegrossi et al., 2016, Panegrossi et al., 2019).
By following a completely different approach, SM2RAIN estimates rainfall starting from SM variations observed by a satellite sensor within a soil layer. The method has been applied to different satellite SM products with satisfactorily results (*Brocca et al., 2014*; *Koster et al., 2016*; *Ciabatta et al., 2018*; *Massari et al., 2017*). Moreover, the integration between SM2RAIN-derived and classical rainfall products was found to provide more reliable data (*Ciabatta et al., 2015, 2017*; *Brocca et al., 2016*; *Tarpanelli et al., 2017*) that can be used also for flood modelling (*Massari et al., 2014*; *Ciabatta et al., 2016*; *Camici et al., 2018*) and landslides forecasting (*Brunetti et al., 2018*).

3 Input data

As stated above, H64 product exploits two different satellite retrieval approaches. The classical top-down approach in which satellites sense clouds from above and the bottom-up approach which is based on SM2RAIN. The two are merged to produce the final rainfall product.

4 Architecture of the product generation chain

The architecture of the H64 product generation chain is shown in Figure 1 and consists of two modules:

1. *Rainfall estimation via SM2RAIN;*
2. *Integration module;*

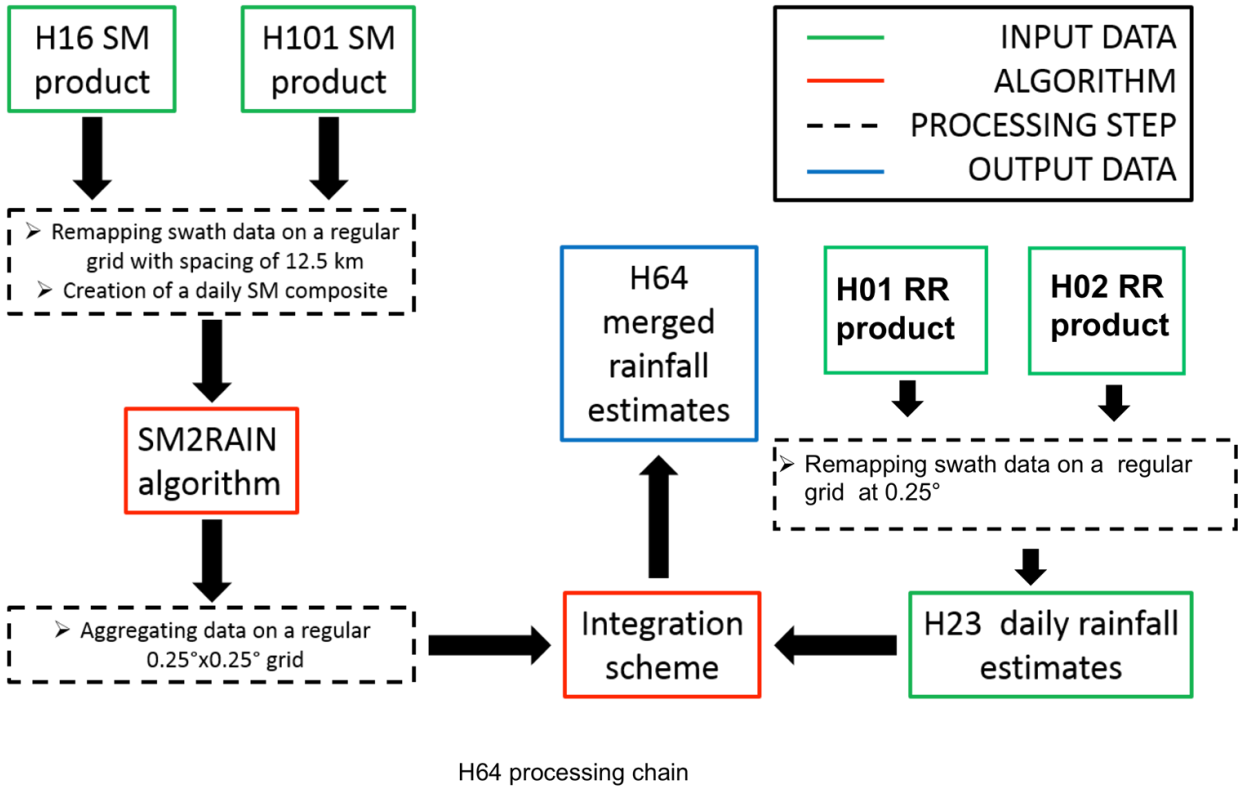

Figure 1 - Architecture of H64 product generation chain

4.1 Rainfall estimation through SM2RAIN

4.1.1 Soil moisture data preprocessing

Before applying SM2RAIN to H16 and H101 SM data, some preprocessing steps are carried out. The H64 algorithm collects all the BUFR files available for the day before the modelling chain run. To do this, all the Product Dissemination Units (PDUs) provided every 3 minutes through MetOp A and B platforms are collected. Then, the swath data are co-located over a 12.5 km grid (the same used for ASCAT Climate Data Record products). In order to reduce the number of spatial and temporal gaps, data provided as H16 and H101 are merged. In case of two coincident SM observations, the average of the two observations is computed. Despite the use of two different SM products, some "holes" can be noticed in the daily composite obtained after every model run, as displayed in Figure 2.

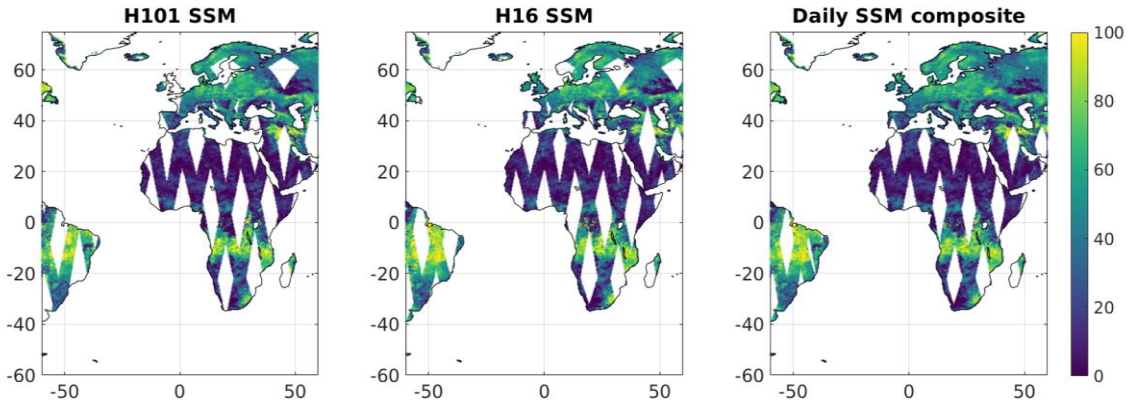

Figure 2 – H101 Soil Moisture data available over the full disk area for the 20th of November 2018 (left panel), H16 Soil Moisture data available or the same day (central panel) and the Soil Moisture Daily Composite obtained by merging the two SM products (right panel).

As it can be observed from Figure 2, both H101 and H16 SM products show blank areas where no retrieval is carried out due to the orbit geometry. These holes are still present in the daily composite but they show reduced areas. For these areas, no rainfall estimation is carried out during the current day.

After these preliminary operations, the H64 algorithm executes the following preprocessing steps:

- all the SM data characterized by a probability of snow at ground or frozen soil higher than 30% are masked out and not used, as these particular conditions can negatively impact the quality of the satellite retrieval;
- all the SM data available in the seven days preceding the algorithm run are collected and collocated over the same 12.5 km grid in order to reduce data gaps by interpolating the SM data at 00:00 UTC;
- the merged observations obtained through the preprocessing steps are then added to the datapool created during the previous operation and interpolated in time at 12:00 UTC and 21:00 UTC. The two interpolations allow to provide rainfall estimation with a latency as short as possible, two different product configurations are provided. The first one uses all the data in the time window 00:00-12:00 UTC of each day (early run), whereas the second one in the time window 00:00-21:00 UTC (late run). In this way, rainfall estimates are available about 2 hours after the last considered satellite soil moisture overpass, i.e. around 14:00 UTC and around 23:00 UTC);
- once the data are added to the datapool, SM observations older than eight days (with respect to the current day), are removed from the ancillary data collection. It is worth noting that in this phase there is no data masking nor flagging.

Due to the limited number of MetOp A and B satellite observations used in the early run, the estimation of rainfall via SM2RAIN is not be possible over a high fraction of the MSG full-disk area. Therefore, the product provided by the algorithm run at 12:00 UTC (early run) is characterized by a lower quality and is not recommended for applications which do not require very short latency observations.
Figure 3 shows the spatial cumulated coverage of MetOp A and B data over the MSG Full-disk area at different temporal interval.

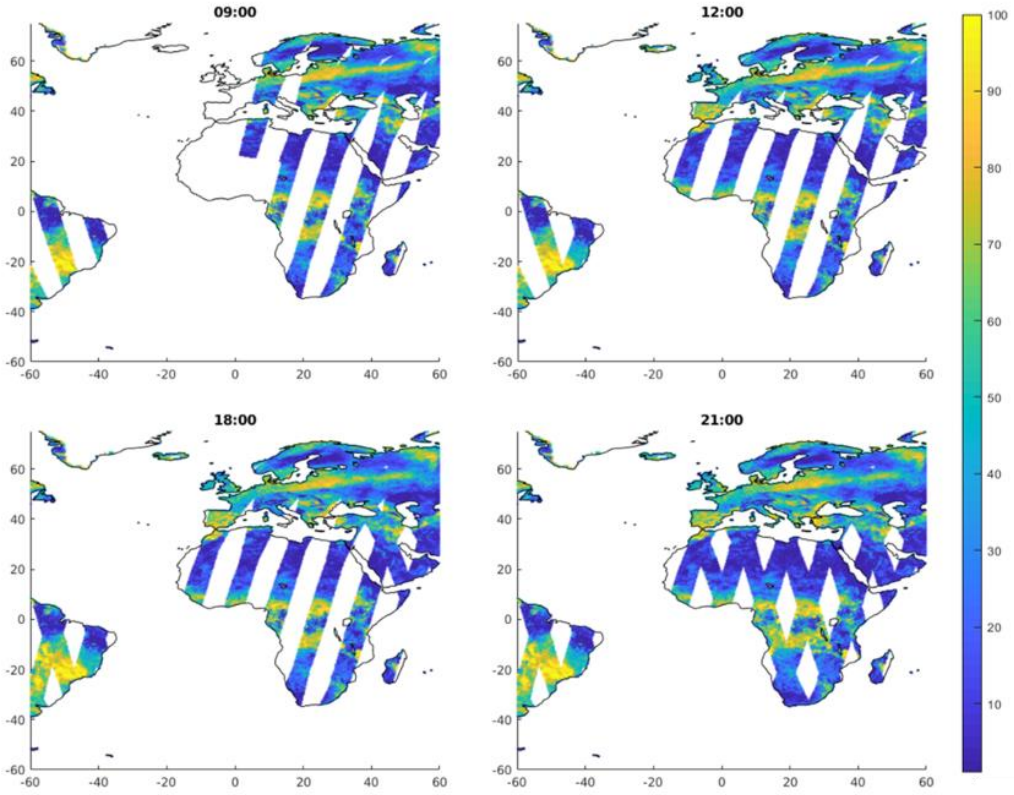

Figure 3 – Spatial coverage obtained by considering all the available MetOp A and B overpasses until 09:00 UTC (upper-left), until 12:00 UTC (upper-right), until 18:00 UTC (bottom-left) and until 21:00 UTC (bottom-right) for a randomly selected day.

4.1.2 The SM2RAIN algorithm

Brocca et al. (2013) proposed an algorithm, namely SM2RAIN, that allows to estimate the amount of rainfall fallen into the soil through soil moisture (SM) observations. The algorithm is based on the inversion of the soil water balance equation:

$$Z^{*}ds(t)/dt = p(t) - r(t) - e(t) - g(t) \quad (1)$$

where *Z** is the soil water capacity (soil depth times soil porosity), *s(t)* is the relative saturation of the soil or relative SM, *t* is the time and *p(t)*, *r(t)*, *e(t)* and *g(t)* are the precipitation, surface runoff, evapotranspiration and drainage rates, respectively. In particular, the drainage rate is calculated by the relationship proposed by *Famiglietti and Wood (1994)*:

$$g(t) = as(t)^b \tag{2}$$

where *a* and *b* are two parameters describing the nonlinearity between the soil saturation and drainage rate (*Brocca et al., 2013*). It is assumed that during rainfall the evapotranspiration rate and the surface runoff are negligible (*Brocca et al., 2015*). Under these assumptions, solving ***Eq. (1)*** for precipitation ends up with the following explicit equation:

$$p(t) = Z^* ds(t)/dt + as(t)^b \tag{3}$$

In summary, once two consecutive observations of SM are available, ***Eq. (3)*** is able to provide an estimate of the rainfall fallen during the time step *dt*.
In order to reduce the effect of noise in the estimated precipitation, an exponential filter was first applied to SM retrievals. As described in *Albergel et al. (2008)*, the filter requires a single parameter, the characteristic time length (*T*), to be calibrated. In the original formulation, the exponential filter allows to estimate the root-zone soil moisture conditions of a deeper layer starting from surface observations. The *T*-value takes into account all the factors affecting the temporal variability of soil moisture, e.g. hydraulic properties, evaporation, and soil layer thickness. The use of such a filter on one hand increases the considered soil layer thickness, thus affecting *Z** parameter, while, on the other hand, reduces the noises contained in the surface SM time series. The *T*-values, along with the SM2RAIN parameters *a*, *b* and *Z** are estimated within the calibration step against a rainfall dataset. The algorithm has been applied successfully on a local (*Brocca et al., 2013; 2015*), regional (*Ciabatta et al., 2015; 2017*) and on a global scale (*Brocca et al., 2014*, *Ciabatta et al., 2018*, *Koster et al., 2016*, *Massari et al., 2017*) to different SM data with good results.

4.1.3 SM2RAIN-based rainfall estimate

The data obtained from the previous preprocessing steps are ready to be used for rainfall estimation through SM2RAIN. The four SM2RAIN parameter values are obtained through calibration. Due to the need of carrying out a rigorous calibration, the parameter values are calibrated by using the H113 SM Data Record product as input. This choice allowed us to perform a long-term calibration during the period 2013-2017 on a global scale, without spatial and/or temporal gaps. The calibration has been carried out by minimizing the daily Root Mean Square Error (RMSE) against ERA5 rainfall product (*Dee et al., 2011*). The calibration has been carried out

on a pixel by pixel basis over the H113 grid (12.5 km). It is worth noting that despite ASCAT SM moisture product is available since 2007, in this application SM2RAIN has been calibrated with the data obtained from the two orbiting platforms (MetOp A and B). In this respect, a new SM2RAIN calibration is foreseen when data of MetOp C will be used for rainfall estimation. On the other hand, when MetOp A will stop working, there will be the need of a new calibration. It was decided to use ERA5 as it is a widely used product and it is considered as a high-quality dataset. Other products (like GPCC or GPM) have not been chosen for the following reasons:

1) GPCC uses ground stations to provide a 1° dataset. While it could be considered of high quality over well instrumented areas, it may fail over regions characterized by a very low gauge density (Massari et al., 2020), and it spatial resolutions is much coarser than ASCAT resolution;
2) GPM provides the users with 3 different products. The Final run uses gauge data to correct satellite estimates, showing the same limitations of ground-based datasets, while the use of satellite-based only rainfall data could introduce additional error in SM2RAIN-derived data as they are characterized by significant uncertainty (please refer to Massari et al. (2020) for a discussion about the best benchmark dataset to use). Moreover, GPM Dual Polarization Radar data can be used to validate H SAF products over area characterized by the absence of ground monitoring network, where the classical validation approach (direct comparison with raingauges and ground radars) it is not possible;

Regarding the limitations of reanalysis datasets (like ERA5) it can be said that they often may fail in representing the variability of convective systems, due to the relatively low resolution and lack of proper parameterization of sub-grid processes (Massari et al., 2020). In the study ERA5, GPCC and a GPM product have been assess through a Triple Collocation (TC) analysis on a global scale during a 4-year period. The analysis showed that ERA5 performed the best, even if it has been underlined higher uncertainties over convective systems. The main findings in terms of correlation coefficient are reported in Table 1.

	A	B	C
GPCC	0.71	0.71	0.70
ERA 5	-	0.81	0.83
IMERG	0.67	0.66	-
SM2RAIN-ASCAT	0.70	-	0.68

Table 1 – Median correlation coefficients obtained through TC analysis for the considered triplets (A, B and C).

This preliminary analysis confirmed the use of ERA 5 as calibration benchmark. For further details about the analysis and the spatial distribution of the performance, the readers are referred to Massari et al. (2020).

Besides these results, in Brocca et al. (2019) the impact of the calibration benchmark selection has been evaluated. In that analysis, SM2RAIN algorithm has been applied to 20000 random satellite pixels. The algorithm parameters have been calibrated against GPCC and ERA 5 to assess the impact of benchmark selection. The analysis showed that the estimated rainfall in the two calibration tests is very similar, with very high correlation coefficients between the two SM2RAIN-derived data records (median value higher than 0.90). This result clearly demonstrates that the selection of the reference dataset has a small influence on SM2RAIN-derived rainfall that is mostly driven from soil moisture temporal fluctuations. For further details about the calibration strategy and SM2RAIN output performance, the readers are referred to Brocca et al. (2019).

Figure 4 shows the spatial distribution of the 4 parameters obtained after the calibration step. The spatial patterns are in good agreement with the physiographic features of the ground. Z* parameter shows higher values in those areas characterized by a more intense rainfall regime, whereas *a* and *b* show higher values in areas characterized by higher impact of drainage (like sandy soils). T is higher where the signal is more impacted by noise.

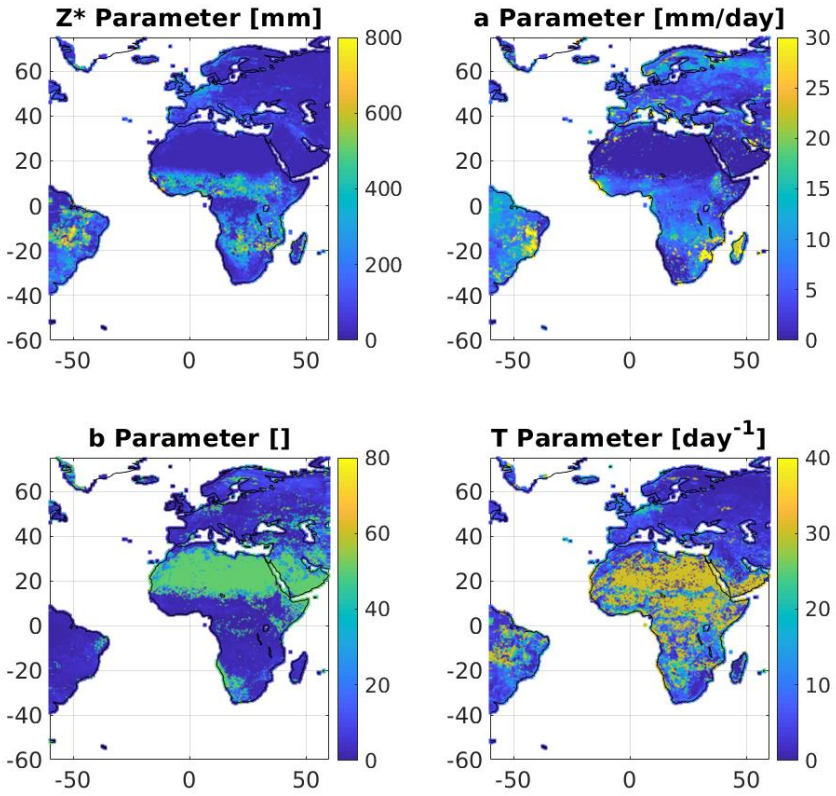

Figure 4 – Z (upper left panel), a (upper right panel), b (bottom left panel) and T (bottom right panel) SM2RAIN parameters spatial distribution within the study area*

4.2 Integration module

Once rainfall is estimated via SM2RAIN according to the procedure described above, the obtained data are resampled over a 0.25°x0.25° regular grid in order to allow the integration with H23.
The regridding is carried out through the application of a simple average of the closest native 12.5 km 8 pixels (inherited from ASCAT grid) to each 0.25° grid points.
After the regridding procedure, SM2RAIN-derived rainfall and H23 data are finally merged. The integration is carried out through a simple linear weighted average between the two products through the following equation:

$$P_{H64} = P_{H23} * (1 - W) + P_{SM2RAIN} * (W) \quad (4)$$

Where P_{H64} is the integrated rainfall, P_{H23} and $P_{SM2RAIN}$ are the rainfall amounts obtained through H23 and SM2RAIN respectively, W is the weight used to integrate the two products. More in details, W ranges between 1 (only SM2RAIN estimates are used to build H64) and 0 (only H23 rainfall data are used to build H64).
The W values have been calibrated on a pixel by pixel basis using the following equation:

$$W = \frac{\sigma_2 * (\rho_{1R} - \rho_{12} * \rho_{2R})}{\sigma_1 * (\rho_{2R} - \rho_{12} * \rho_{1R}) + \sigma_2 * (\rho_{1R} - \rho_{12} * \rho_{2R})} \quad (5)$$

Where σ and ρ are the standard deviation and the Pearson's correlation coefficient of the two parent products (H23 and SM2RAIN-derived rainfall) and the benchmark. In this case the calibration of the weights has been carried out against ERA5 during the period 2011-2014. The use of eq. 5 should limit the impact of using the same calibration dataset, ERA5, for estimating the integration weights. Moreover, the impact of the calibration dataset should be limited. In Brocca et al., 2020, the use of two different calibration benchmarks was tested showing that the differences between the two obtained datasets were negligible, suggesting a limited impact of the calibration benchmark. The spatial distribution of the integration weights over land is displayed in Figure 5.

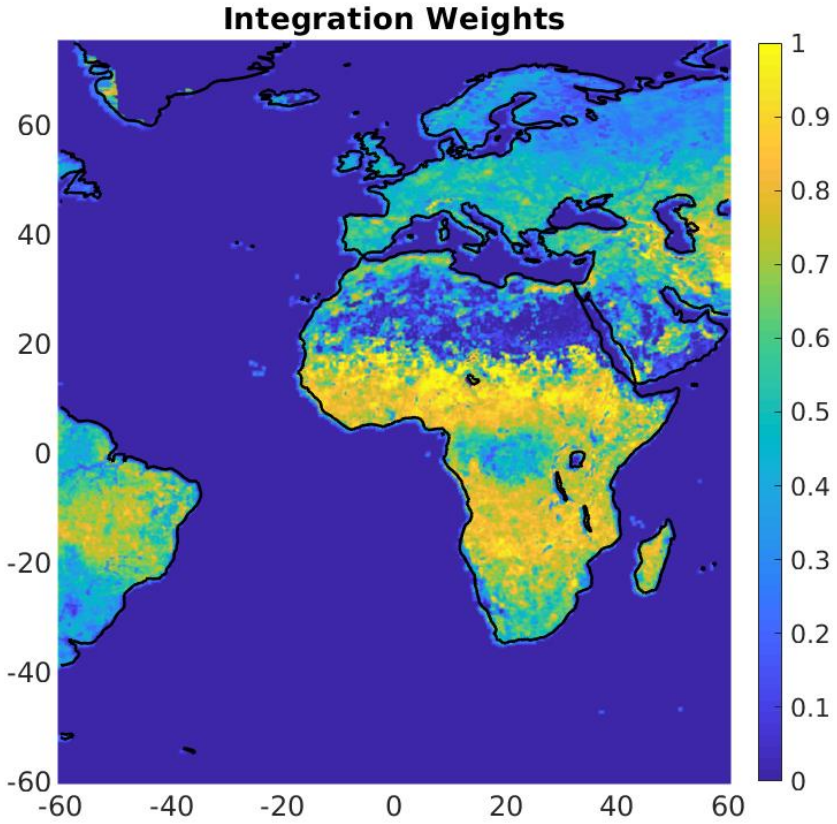

Figure 5 – *Spatial distribution of the integration weights used for the merging of H23 and SM2RAIN-derived rainfall.*

As it can be observed in Figure 5, the integration weights are lower (more weight given to H23) where SM input data are characterized by a lower quality (over deserts, tropical forests, high latitudes). In the current version of the algorithm the integration weights are static in time but it is foreseen to adopt a dynamic merging technique as soon as a longer data period can be used for calibration. This will allow to define weights varying as function of vegetation or seasons. As stated above, SM2RAIN is able to retrieve rainfall only over land and thus, rainfall over oceans is provided only by H23. This aspect can create some artifacts in rainfall estimation due to the use of a single product offshore (H23) whereas, on coast pixels, the estimated rainfall is the outcome of the integration scheme. In order to avoid high differences at the water/land interface, all the coastal pixels are characterized by an integration weight smaller than the calibrated one:

$$W_{coast} = \frac{W}{2} \quad (6)$$

At the same time, a buffer zone of 0.25° (one pixel) is created between coasts and oceans. The buffer zone is used to define integration weights even smaller than the coastal ones:

$$W_{buffer} = W/4 \quad (7)$$

The spatial distribution of coastal and buffer pixels is reported in Figure 6.

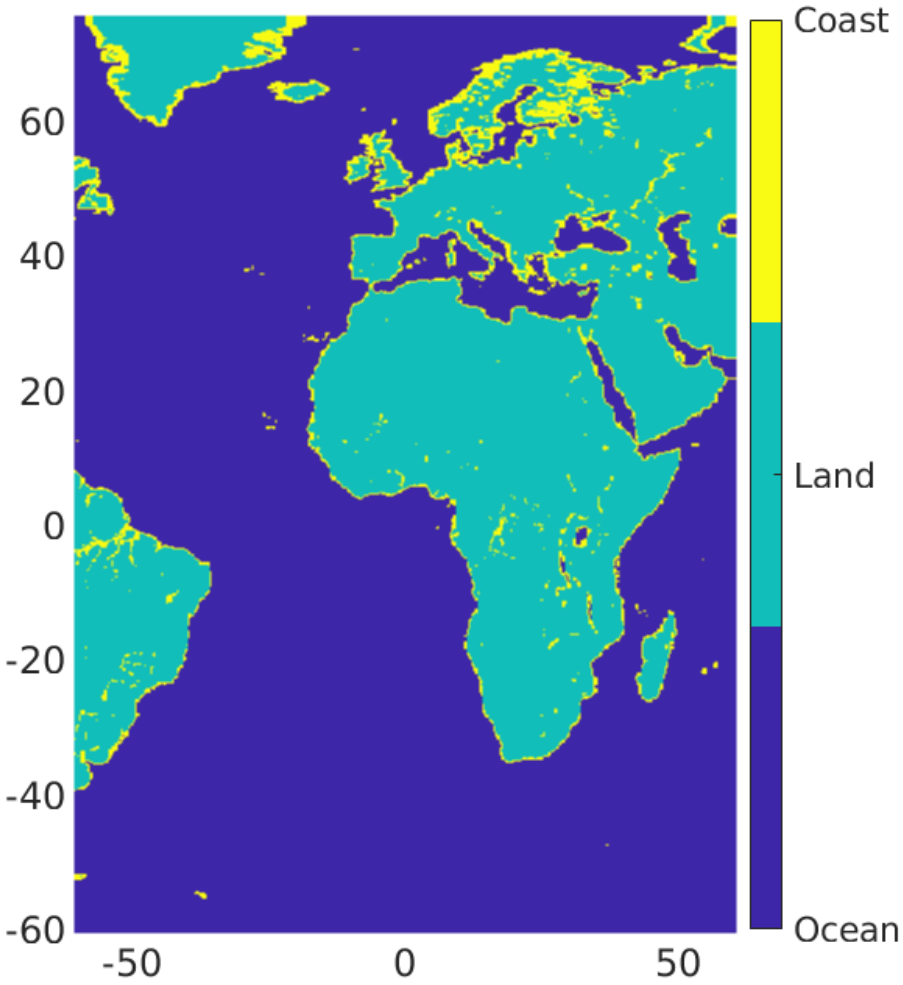

Figure 6 – *Land/ocean/coast mask used to create the buffer zone along the coastline.*

Figure 7 shows an example of the rainfall integration for the H64 product generation. Moreover, over the blank areas identified by the "diamonds" in Figure 3, no integration is carried out and only rainfall estimates obtained through H23 are used to generate H64. At the edge of these areas, the same weighting factor adjustment has been applied.

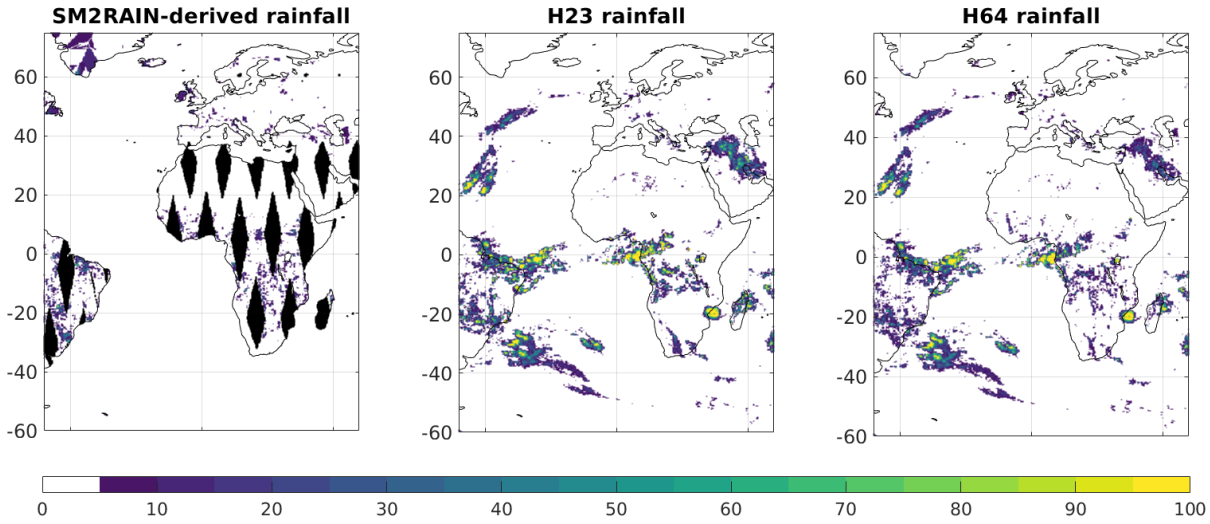

Figure 7 – *Example of rainfall generation (in mm/d) through SM2RAIN (left panel), H23 rainfall estimates (middle panel) and H64 integrated rainfall product (right panel).*

4.3 Output files

The H64 product is provided in NetCDF format. Each output file contains latitude, longitude, daily rainfall and an integration flag showing which product has been used for obtaining the final estimate.
More in details, each file is characterized by:

- nlat: 540 (Number of 0.25° grid intervals of latitude from 75° N to 60° S).
- nlon: 480 (Number of 0.25° grid intervals of longitude from 60°W to 60°E).

Variable definitions:

- *Rainfall*: daily precipitation in mm
- *Integration flag*: shows which product has been used for the integration according to Table .

The general format of output file names is the following:
*h64*_<Date>.<Extension>, where

i. Date contains a four-digit year, a two-digit month, and a two-digit day (YYYYMMDD);
ii. Extension is nc (NetCDF 4).

Example:
h64_20151214.nc

Flag Value	Products used for H64 generation
0	H23 and SM2RAIN-derived rainfall
1	H23 only
2	SM2RAIN only
3	No available data

Table 2 - Integration flag definition

It is worth noting that all international agencies delivering operational PMW precipitation products in terms of both Level 2 (orbital) and Level 3 (gridded daily or monthly) products. The advantage of delivering a Level 3 PMW daily precipitation product within H-SAF is twofold:

1. the gridded product can be well exploited for hydrological applications and for data assimilation in hydrological models;
2. the product can be easily compared to global rainfall gridded datasets (i.e., GPCP) and to similar PMW Level 3 daily (and monthly) estimates provided by other international agencies (i.e., NASA with GPROF Level 3 daily and monthly mean at 0.25°x0.25° resolutions, or NOAA MiRS Level 3 products).

5 Applications and evaluation of H64 product

H64 daily rainfall product, taking advantage of the integration between the bottom-up and top-down approaches, provides valuable and reliable estimates that can be used with benefit for hydrological applications. The integration between top-down and bottom-up approaches has been already tested and assessed in Italy (*Ciabatta et al., 2017*). In this study a prototype version of H64 has been created by merging a satellite microwave precipitation product and SM2RAIN-derived rainfall. Then the product has been evaluated against observed data in Italy with very satisfactorily results, in terms of Correlation coefficient (R) and Root Mean Square Error (RMSE). The main findings of that study are summarized in Figure 8. As it can be observed, the integration provides a strong improvement both in terms of R and RMSE with respect to the parent products alone.

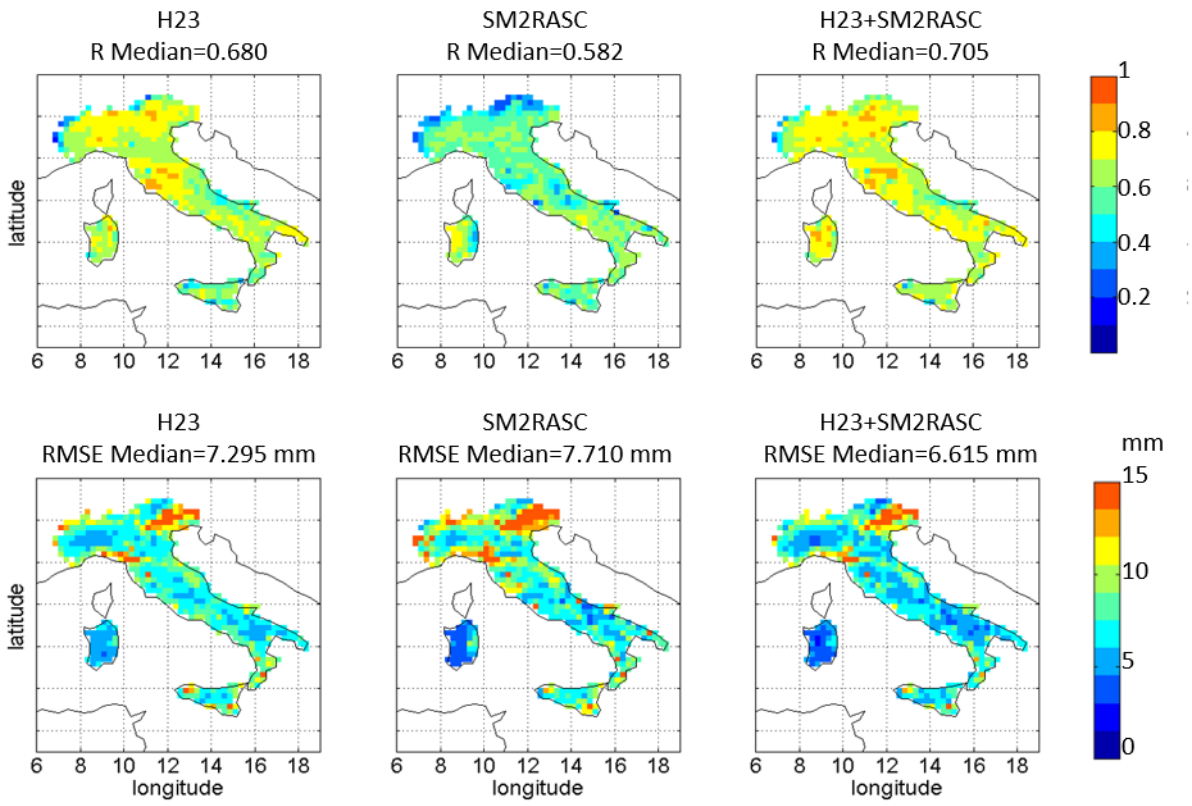

Figure 8 – *R (upper panel) and RMSE maps (lower panel) obtained by comparing H23 product (right), SM2RAIN-derived rainfall (middle) and the combination of the two products (left).*

Recently, H64 has been tested also as input for flood modelling. Here an application of H64 as input for flood modelling is briefly presented and discussed. This analysis has been carried out over 720 basins in Europe with area ranging between 200 to 160000 km^2 during the period 2011-2014. The H64 rainfall data are used to force the MISDc rainfall-runoff model (*Brocca et al., 2011*) in order to simulate discharge. The performances are evaluated in terms of Kling-Gupta Efficiency Index (KGE) against observed discharge data, KGE has a perfect score of 1, while values lower than 0 highlight unsatisfactory model results. KGE is defined as:

$$KGE = 1 - \sqrt{(r-1)^2 + \left(\frac{\sigma_{sim}}{\sigma_{obs}} - 1\right)^2 + \left(\frac{\mu_{sim}}{\mu_{obs}} - 1\right)^2} \quad (7)$$

where r is the linear correlation between simulated (sim) and observed (obs) data, σ is the standard deviation and μ is the mean of the simulated and observed discharge values.
In order to assess the results provided by H64, the analysis has been carried out also by forcing the model with a ground-based dataset (EOBS, *Cornes et al., 2018*), and with a state-of-the-art satellite rainfall product (TMPA, *Huffman et al., 2007*) and by considering H23 parent product

alone. Results in terms of KGE are displayed in Figure 9. As it can be noticed, H64 rainfall estimates provided very good results over the analyzed catchments. The integration provided a high improvement with respect of H23, especially in Central Europe and Spain. H64 provided better results than those obtained by forcing the model with TMPA data, almost over all the analysis domain, confirming the added value of integrating multiple sources of information. The skill of reproducing observed discharge is very close to the ground-based dataset EOBS. This aspect is of paramount importance as H64 could be released with a small latency, providing a reliable rainfall dataset that can be used for operational hydrological applications.

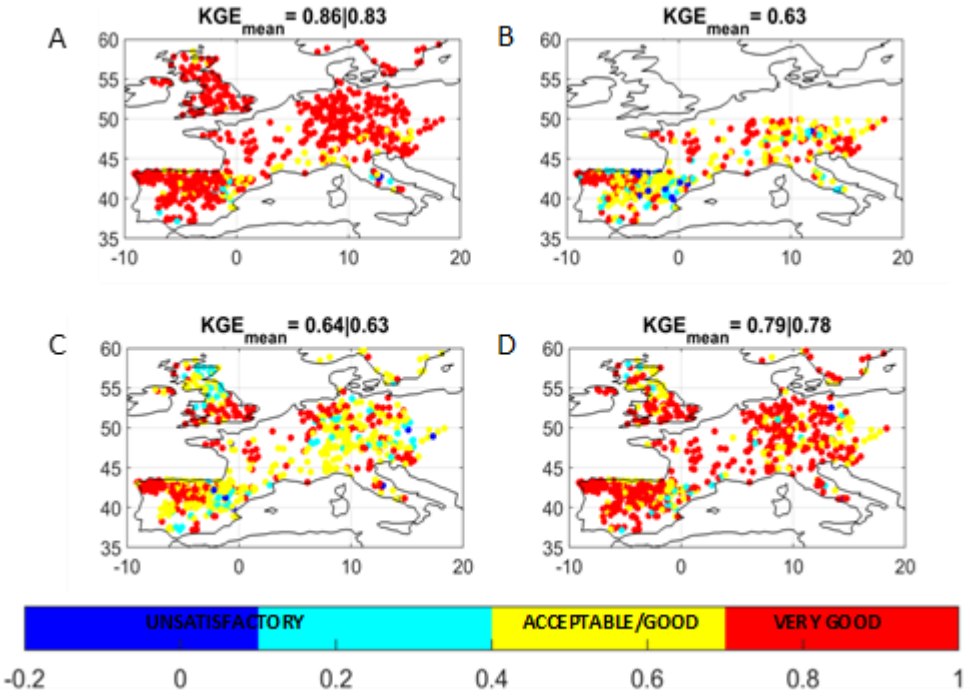

Figure 9 – *Hydrological validation carried out over the European area by considering EOBS (A), TMPA (B), H23 (C) and H64 (D). the results are expressed in terms of KGE.*

6 References

Albergel, C., Rudiger, C., Pellarin, T., Calvet, J.C., Frtiz, N., Froissard, F., Suquia, D., Petitpa, A., Piguet, B., Martin, E. (2008). From near-surface to root-zone soil moisture using an exponential filter: An assessment of the method based on in-situ observations and model simulations. Hydrol. Earth Syst. Sci., 12, 1323-1337.

Brocca, L., Melone, F., Moramarco, T. (2011). Distributed rainfall-runoff modelling for flood frequency estimation and flood forecasting. Hydrological Processes, 25 (18), 2801-2813.

Brocca, L., Melone, F., Moramarco, T., Wagner, W. (2013). A new method for rainfall estimation through soil moisture observations. Geophys. Res. Lett., 40(5), 853-858.

Brocca, L., Ciabatta, L., Massari, C., Moramarco, T., Hahn, S., Hasenauer, S., Kidd, R., Dorigo, W., Wagner, W., Levizzani, V. (2014). Soil as a natural rain gauge: estimating global rainfall from satellite soil moisture data. Journal of Geophysical Research Atmosphere, 119(9), 5128-5141.

Brocca, L., Massari, C., Ciabatta, L., Moramarco, T., Penna, D., Zuecco, G., Pianezzola, L., Borga, M., Matgen, P., Martínez-Fernández, J. (2015). Rainfall estimation from in situ soil moisture observations at several sites in Europe: an evaluation of SM2RAIN algorithm. Journal of Hydrology and Hydromechanics, 65, 3, 201-209.

Brocca, L., Filippucci, P., Hahn, S., Ciabatta, L., Massari, C., Camici, S., Schüller, L., Bojkov, B., Wagner, W. (2019). SM2RAIN-ASCAT (2007-2018): global daily satellite rainfall from ASCAT soil moisture. Earth System Science Data, 11, 1583–1601, doi:10.5194/essd-11-1583-2019. https://doi.org/10.5194/essd-11-1583-2019.

Brunetti, M.T., Melillo, M., Peruccacci, S., Ciabatta, L., Brocca, L. (2018). How far are we from the use of satellite data in landslide forecasting? Remote Sensing of Environment, 210, 65-75, doi:10.1016/j.rse.2018.03.016

Camici, S., Ciabatta, L., Massari, C., Brocca, L. (2018). How reliable are satellite precipitation estimates for driving hydrological models: a verification study over the Mediterranean area. Journal of Hydrology, 563, 950-961.

Casella, D., Panegrossi, G., Sanò, P., Mugnai, A., Smith, E. A., Tripoli, G. J., Dietrich, S., Formenton, M., Leung, W.Y., and Mehta, A.: Transitioning from CRD to CDRD in bayesian retrieval of rainfall from satellite passive microwave measurements: Part 2. Overcoming database profile selection ambiguity by consideration of meteorological control on microphysics, IEEE T. Geosci. Remote, 51, 4650-4671, 2013.

Casella D., L. M. Amaral, S. Dietrich, A. C. Marra, P. Sanò, and G. Panegrossi, 2017: The Cloud Dynamics and Radiation Database algorithm for AMSR2: exploitation of the GPM observational dataset for operational applications. IEEE J. of Sel. Topics in Appl. Earth Obs. and Rem. Sens., 10, 3985 - 4001, doi:10.1109/JSTARS.2017.2713485.

Ciabatta, L., Brocca, L., Massari, C., Moramarco, T., Gabellani, S., Puca, S., Rinollo, A., Wagner, W. (2015). Integration of satellite soil moisture and rainfall observations over the Italian territory. Journal of Hydrometeorology, 16(3), 1341-1355.

Ciabatta, L., Brocca, L., Massari, C., Moramarco, T., Gabellani, S., Puca, S., Wagner, W. (2016). Rainfall-runoff modelling by using SM2RAIN-derived and state-of-the-art satellite rainfall products over Italy. International Journal of Applied Earth Observation and Geoinformation, 48, 163-173.

Ciabatta, L., Marra, A.C., Panegrossi, G., Casella, D., Sanò, P., Dietrich, S., Massari, C., Brocca, L. (2017). Daily precipitation estimation through different microwave sensors: verification study over Italy. Journal of Hydrology, 545, 436-450.

Ciabatta, L., Massari, C., Brocca, L., Gruber, A., Reimer, C., Hahn, S., Paulik, C., Dorigo, W., Kidd, R., Wagner, W. (2018). SM2RAIN-CCI: a new global long-term rainfall data set derived from ESA CCI soil moisture. Earth System Science Data, 10, 267-280.

Cornes, R., G. van der Schrier, E.J.M. van den Besselaar, and P.D. Jones. (2018). An Ensemble Version of the E-OBS Temperature and Precipitation Datasets, J. Geophys. Res. Atmos., 123. doi:10.1029/2017JD028200

Dee, D. P., Uppala, S. M., Simmons, A. J., Berrisford, P., Poli,P., Kobayashi, S., Andrae, U., Balmaseda, M. A., Balsamo, G.,Bauer, P., Bechtold, P., Beljaars, A. C. M., van de Berg, L., Bid-lot, J., Bormann, N., Delsol, C., Dragani, R., Fuentes, M., Geer,A. J., Haimberger, L., Healy, S. B., Hersbach, H., Holm, E. V.,Isaksen, L., Kallberg, P., Kohler, M., Matricardi, M., McNally, A.P., Monge-Sanz, B. M., Morcrette, J. J., Park, B. K., Peubey, C.,de Rosnay, P., Tavolato, C., Thepaut, J. N., and Vitard, F. (2011). The ERA-Interim reanalysis: configuration and performance of the data assimilation system, Q. J. Roy. Meteor. Soc., 137, 553–597.

Ebert, E. E., Janowiak, J. E., Kidd, C. (2007). Comparison of near-real-time precipitation estimates from satellite observations and numerical models. Bull. Amer. Meteor. Soc., 88, 47–64, doi:10.1175/BAMS-88-1-47.

Famiglietti J.S., Wood E.F. (1994). Multiscale modeling of spatially variable water and energy balance processes. Water Resources Research, 11, 3061-3078.

Huffman, G.J., Adler, R.F., Bolvin, D.T., Gu, G., Nelkin, E.J., Bowman, K.P., Hong, Y., Stocker, E.F., Wolff, D.B. (2007). The TRMM Multisatellite Precipitation Analysis (TMPA): Quasi global, multiyear, combined-sensor precipitation estimates at fine scales. J. Hydrometeor., 8(1), 38-55.

Kidd, C., Levizzani, V. (2011). Status of satellite precipitation retrievals. Hydrol. Earth Syst. Sci., 15, 1109-1116.

Koster, R.D., Brocca, L., Crow, W.T., Burgin, M.S., De Lannoy, G.J.M. (2016). Precipitation Estimation Using L-Band and C-Band Soil Moisture Retrievals. Water Resources Research, 59(9), 7213-7225.

Marra, A. C., D. Casella, P. Sanò, G. Panegrossi, M. Petracca, S. Dietrich, and V. Levizzani, 2015: Analysis and comparison of global precipitation datasets with gridded products from passive microwave retrieval algorithms in the GPM era. Earth Observation for Water Cycle Science, Frascati, 20-23 Oct., http://congrexprojects.com/custom/15C10/D2_1045_Marra.pdf

Massari, C., Brocca, L., Moramarco, T., Tramblay, Y., Didon Lescot, J.-F. (2014). Potential of soil moisture observations in flood modelling: estimating initial conditions and correcting rainfall. Advances in Water Resources, 74, 44-53.

Massari, C., Crow, W., Brocca, L. (2017). An assessment of the accuracy of global rainfall estimates without ground-based observations. Hydrology and Earth System Sciences, 21, 4347-4361.

Massari, C., Brocca, L., Pellarin, T., Abramowitz, G., Filippucci, P., Ciabatta, L., Maggioni, V., Kerr, Y., Fernández-Prieto, D. (2020). A daily/25km short-latency rainfall product for data scarce regions based on the integration of the GPM IMERG Early Run with multiple satellite soil moisture products. Hydrology and Earth System Sciences, in press, doi:10.5194/hess-2019-387. https://doi.org/10.5194/hess-2019-387.

Mugnai, A., Smith, E. A., Tripoli, G. J., Bizzarri, B., Casella, D., Dietrich, S., Di Paola, F., Panegrossi, G., and Sanò, P.: CDRD and PNPR satellite passive microwave precipitation retrieval algorithms:

euroTRMM/EURAINSAT Origins and H-SAF operations, Nat. Hazards Earth Syst. Sci, 13, 887–912, 2013.

Panegrossi G., D. Casella, S. Dietrich, A. C. Marra, L. Milani, M. Petracca, P. Sanò, A. Mugnai (2014). CDRD and PNPR passive microwave precipitation retrieval algorithms: extension to the MSG full disk area, Proc. 2014 EUMETSAT Meteorological Satellite Conference, Geneva, Sept. 2014,https://www.eumetsat.int/website/home/News/ConferencesandEvents/DAT_2076129.html

Panegrossi G., D. Casella, S. Dietrich, A. C. Marra, M. Petracca, P. Sanò, A. Mugnai, L. Baldini, N. Roberto, E. Adirosi, R. Cremonini, R. Bechini, G. Vulpiani, and F. Porcù: Use of the GPM constellation for monitoring heavy precipitation events over the Mediterranean region, IEEE J. of Sel. Topics in Appl. Earth Obs. and Rem. Sens. (J-STARS), Volume 9, Issue 6, Pages: 2733 - 2753, doi: 10.1109/JSTARS.2016.2520660, 2016.

Panegrossi, G.; Marra, A.C.; Sanò, P.; Baldini, L.; Casella, D.; Porcù, F. Heavy precipitation systems in the Mediterranean area: The role of GPM. In: Satellite precipitation measurement.; Satellite precipitation measurement.; Springer.; V. Levizzani, C. Kidd, D. B. Kirschbaum, C. D. Kummerow, K. Nakamura, F. J. Turk, Eds.: Dordrecht, 2019, in press.

Sanò, P., Casella, D., Mugnai, A., Schiavon, G., Smith, E. A., and Tripoli, G. J.: Transitioning from CRD to CDRD in bayesian retrieval of rainfall from satellite passive microwave measurements: Part 1. Algorithm description and testing, IEEE T. Geosci. Remote, 51, 4119-4143, doi: 10.1109/TGRS.2012.2227332, 2013.

Sanò, P., Panegrossi, G., Casella, D., Di Paola, F., Milani, L., Mugnai, A., Petracca, M., and Dietrich, S.: The Passive microwave Neural network Precipitation Retrieval (PNPR) algorithm for AMSU/MHS observations: description and application to European case studies, Atmos. Meas. Tech., 8, 837–857, doi:10.5194/amt-8-837-2015, 2015.

Sanò, P., G. Panegrossi, D. Casella, A. C. Marra, F. Di Paola, and S. Dietrich, “The new Passive microwave Neural network Precipitation Retrieval (PNPR) algorithm for the cross-track scanning ATMS radiometer: Description and verification study over Europe and Africa using GPM and TRMM spaceborne radars,” Atmos. Meas. Techn., vol. 9, pp. 5441–5460, 2016. Doi: 10.5194/amt-9-5441.

Skofronick-Jackson, G.; Petersen, W.A.; Berg, W.; Kidd, C.; Stocker, E.F.; Kirschbaum, D.B.; Kakar, R.; Braun, S.A.; Huffman, G.J.; Iguchi, T.; et al. The Global Precipitation Measurement (GPM) Mission for Science and Society. Bull. Am. Meteorol. Soc. 2017, 98, 1679–1695.

Tarpanelli, A., Massari, C., Ciabatta, L., Filippucci, P., Amarnath, G., Brocca, L. (2017). Exploiting a constellation of satellite soil moisture sensors for accurate rainfall estimation. Advances in Water Resources, 108, 249-255.

ATBD (2016): “Algorithm Theoretical Baseline Document (ATBD) Surface Soil Moisture ASCAT NRT Orbit” Tech. Rep. Doc. No: SAF/HSAF/CDOP2/ATBD/, v0.2, 2016.

ATBD (2013a): “Algorithm Theoretical Baseline Document (ATBD) for product H01 new rel.” Tech. Rep. Doc. No: SAF/HSAF/ATBD-01new rel., v2.1, 2013.

ATBD (2013b): “Algorithm Theoretical Baseline Document (ATBD) for product H02b new rel.” Tech. Rep. Doc. No: SAF/HSAF/ATBD-02Anew rel., v2.1, 2013.